

Interactions between integrin $\alpha 9\beta 1$ and VCAM-1 promote neutrophil hyperactivation and mediate poststroke DVT

Short title: NEUTROPHIL INTEGRIN $\alpha 9$ PROMOTES POSTSTROKE DVT

Nilesh Pandey¹, Harpreet Kaur¹, Mehul R Chorawala², Sumit Kumar Anand¹, Lakshmi Chandaluri¹, Megan E Butler³, Richa Aishwarya¹, Shiva J. Gaddam⁴, Xinggui Shen¹, Mabruka Alfaidi⁵, Jian Wang⁶, Xiaolu Zhang⁶, Kavitha Beedupalli⁴, Md. Shenuarin Bhuiyan^{1,3}, Mohammad Alfrad Nobel Bhuiyan⁷, Prabandh Buchhanolla⁸ Prashant Rai⁸, Rahul Shah⁸, Himanshu Chokhawala⁸, J. Dedrick Jordan⁸, Tarek Magdy¹, A Wayne Orr^{1,3}, Karen Y Stokes³, Oren Rom^{1,3}, and Nirav Dhanesha¹

¹Department of Pathology and Translational Pathobiology, Louisiana State University Health Sciences Center-Shreveport, Shreveport, LA 71103, USA.

²Department of Pharmacology and Pharmacy Practice, L. M. College of Pharmacy, Opp. Gujarat University, Ahmedabad, Gujarat, 380009

³Department of Molecular and Cellular Physiology, Louisiana State University Health Sciences Center at Shreveport, Shreveport, USA.

⁴Department of Hematology and Oncology and Feist Weiller Cancer Center, Louisiana State University Health Sciences Center-Shreveport, Shreveport, LA, USA.

⁵Department of Internal Medicine, Division of Cardiology, Center for Cardiovascular Diseases and Sciences, Louisiana State University Health Sciences Center at Shreveport, Shreveport, USA.

⁶Bioinformatics and Modeling Core, The Center for Applied Immunology and Pathological Processes, Department of Microbiology and Immunology, Louisiana State University Health Sciences Center, Shreveport, LA, USA.

⁷Department of Medicine, Louisiana State University Health Sciences Center at Shreveport, Shreveport, USA.

⁸Department of Neurology, Louisiana State University Health Sciences Center at Shreveport, Shreveport, USA.

Mice

To generate neutrophil-specific $\alpha 9$ deficient mouse ($\alpha 9^{\text{fl/fl}}$ Mrp8Cre^{+/-}), $\alpha 9^{\text{fl/fl}}$ mouse was crossed with Mrp8Cre^{+/-} mouse (Supplemental Figure 2A), as we recently reported.¹ Littermates ($\alpha 9^{\text{fl/fl}}$ Mrp8Cre^{-/-}) were used as controls. Mice were genotyped by PCR according to protocols from

the Jackson laboratory. Mice were kept in standard animal house conditions with controlled temperature and humidity and had ad libitum access to standard chow diet and water. The LSU Health Shreveport Animal Care and Use Committee approved all the procedures and studies were performed according to the current Animal Research: Reporting of In Vivo Experiment guidelines (<https://www.nc3rs.org.uk/arriveguidelines>).

Inferior vena cava (IVC) stenosis and stasis model for DVT

The mouse IVC stenosis model of DVT was performed, as reported.²⁻⁵ Only male mice were used for this model, as ligation in female mice may result in necrosis of the reproductive organs.^{4,6} Briefly, a midline laparotomy was made, IVC side branches were first ligated. For stenosis, a space holder (30-gauge) was positioned on the outside of the exposed IVC, and a permanent narrowing ligature was placed below the left renal vein. Next, the needle was removed to restrict blood flow to 80-90%. IVC thrombi were harvested 48-hour post-stenosis, detached from the vessel wall, dried, and weighed in a microbalance, and imaged. The operator was blinded with respect to the genotype and treatment of mice. Mice with surgery time more than 10 mins and mice with accidental bleeding during surgery were excluded. Only mice that exhibited thrombosis were included to quantify the thrombus weight.

For stasis, IVC and all the visible side branches were completely ligated and IVC thrombi were harvested 48-hour post-stasis.

Post-stroke DVT mouse model

The embolic stroke model was performed as previously described by us.^{7,8} Briefly, an autologous embolus clot was prepared using arterial blood was supplemented with human fibrinogen (2 mg/ml, Sigma, #F3879) and immediately clotted in a PE-50 tube for 4 hours at room temperature, followed by storage at 4°C overnight. On the following day, the blood clot was washed in PBS by several passages from a PE-10 tube and transferred to a modified PE-10 catheter. Animals were anesthetized with 1–1.5% isoflurane during the surgery. The catheter containing a single 10 mm fibrin-rich clot was then introduced into the external carotid artery and advanced to the internal carotid artery. After the embolization, the catheter was removed, and the external carotid artery was blocked by cauterization. Laser Doppler flow monitoring was used to confirm the induction of ischemia. Throughout the surgery, the body temperature of the mice was maintained at 37°C ± 1.0 using a heating pad. DVT was induced by IVC stenosis, 1 hour post-stroke and

thrombosis was evaluated after 48 hours, as reported by us.² Only mice that exhibited thrombosis were included to quantify the thrombus weight.

Mouse bone-marrow neutrophil isolation

Bone-marrow neutrophils were isolated using density gradient method as reported by us.⁷⁻¹⁰ Briefly, under sterile conditions, bone marrow cells were extracted from excised femurs and tibiae of euthanized donor mice. Bone marrow cells were gently loaded onto a discontinuous Histopaque gradient (Sigma #1077 and #1119), and centrifuged at 700×g for 30 min, RT, without brake. Neutrophils were collected from the interface between the Histopaque buffers. Red blood cells were eliminated by hypotonic lysis. Neutrophil purity was determined by flow cytometry and found consistently to be > 90%.

Human samples collection and neutrophils isolation

Peripheral blood was collected at the LSUHS-Shreveport from healthy volunteers and patients with stroke (approved IRB protocol, #0002176). Samples were processed within 15 minutes from their collection, and neutrophils were isolated as we previously reported.⁸ Briefly, peripheral venous blood was collected into sodium citrate blood collection tubes, incubated for 20 min at room temperature with 5:1 volume of HetaSep (StemCell # 07806) to allow red blood cell sedimentation. The upper layer was then gently loaded on top of Histopaque-1077 and centrifuged at 400×g, 30 min, RT, no brake. A pellet, containing the neutrophils and RBCs, was further subjected to red blood cell lysis. Neutrophil purity was determined by flow cytometry and found consistently to be > 90%.

ELISA assay

Plasma VCAM-1 was analyzed using commercially available kits (Human VCAM-1/CD106 Quantikine ELISA Kit, R&D systems # DVC00 and Mouse VCAM-1/CD106 Quantikine ELISA Kit, R&D systems # MVC00). Elastase and MPO from plasma and cell supernatant were analyzed using commercially available kits (Mouse Neutrophil Elastase/ELA2 Quantikine ELISA Kit, R&D systems # MELA20 and Mouse Myeloperoxidase DuoSet ELISA, R&D systems # DY3667).

RNA sequencing and data analysis

Neutrophil cell-pellets were lysed, and RNA was isolated using the RNeasy Mini Kit (Qiagen #74106) as per manufacturer's instructions. Libraries were prepared with the Stranded mRNA Prep, Ligation Kit (Illumina). One μg of RNA was processed for each sample and mRNA was purified and fragmented. cDNA was synthesized, and 3' ends were adenylated. Anchor sequences were ligated to each sample and a limited-cycle PCR was performed to amplify and index the libraries. The average library size was determined using an Agilent TapeStation D1000 assay (Agilent Technologies) and libraries were quantitated with qPCR (Bio-rad CFX96 Touch Real-Time PCR, NEB Library Quant Kit for Illumina). Libraries were normalized to 0.5 nM and pooled. The library pool was denatured and diluted to approximately 100pM. A 1% library of 2.5pM PhiX was spiked in as an internal control. Paired end 76 x 76 base pair sequencing was performed on an Illumina NovaSeq 6000. Primary analysis, including base calling and quality scoring, was performed onboard the Illumina NovaSeq 6000 (NovaSeq Control Software v1.8.0; RTA v3). Samples were de-multiplexed, the adapter sequences were removed (the first 9 cycles of sequencing were trimmed), and FASTQ files were generated. Data analysis was performed as we previously described. The quality of the raw FASTQ files was checked through FastQC v0.11.8 (<https://www.bioinformatics.babraham.ac.uk/projects/fastqc/>). Trimmomatic v.0.35 was used to trim the low-quality reads with the parameters: SLIDINGWINDOW:4:20 MINLEN:25. The resulted high-quality reads were then mapped to the mouse reference genome (GRCm38.90) using STAR 2.5.1b¹¹ and quantified by RSEM 1.2.31¹² following the ENCODE-DCC/RNA-seq pipeline. Differentially expression analysis was performed using Bioconductor limma + Voom (Version: 3.48.3) and EdgeR (Version: 3.34.1) packages.^{13,14} Benjamini-Hochberg correction was used to obtain adjusted p-values. Statistically significant differentially expressed genes were filtered based on adjusted $p < 0.01$. Genes with adjusted P value < 0.01 were considered as significant DEGs. The upregulated and downregulated DEGs were analyzed for significantly enriched Gene Ontology pathways using the clusterProfiler package (version 4.8.3). The significance of the enrichment was determined by right-tailed Fisher's exact test followed by Benjamini-Hochberg multiple testing adjustment. The heatmap of all shared DEG between stimulated vs unstimulated and KO vs control (Figure 4H) was generated by ComplexHeatmap R package (version 2.16.0). Hierarchical clustering of top 100 differentially expressed genes (supplementary figure 6 A and B) was visualized as a heatmap using R package gplots (version 3.1.3).

RNA isolation and quantitative real time PCR

RNA was isolated using the RNeasy Mini Kit (Qiagen #74106) as per manufacturer's instructions. cDNA was synthesized using the SuperScript III First-Strand Synthesis System (Invitrogen #18080-051) as per manufacturer's instructions. cDNA synthesis was performed in a Mastercycler nexus gradient thermocycler (Eppendorf). Primers were purchased from Integrated DNA Technologies (Supplementaal Table 2) and qRT-PCR was performed using SSoAdvanced Universal SYBR Green Supermix (Bio-Rad #175271) with a CFX96 Touch Real-Time PCR Detection System (BioRad) according to manufacturer's instructions. Results were normalized to housekeeping genes (*Gapdh* or *Actb*) and expressed as a fold change from control treatments using the $\Delta\Delta C_t$ threshold cycle method of normalization.

Identification of perturbagens altering gene expression for pharmacogenomics profiling

The Library of Integrated Network-Based Cellular Signatures (LINCS) is a National Institute of Health initiative that aims to create a comprehensive network of molecular reactions in response to environmental and internal stressors.¹⁵ The LINCS project uses the L1000 assay, a gene expression array of 978 "hub" genes, to generate gene signatures. The L1000 genes are a reduced representation of the transcriptome, accounting for ~82% of the information content of the transcriptome.¹⁶ The LINCS database contains hundreds of thousands of gene signatures generated in human cell lines treated with chemical perturbagens (drugs) or following knockout or overexpression of individual genes. The $\log_2(\text{fold-change})$ (logFC) and p-value for L1000genes were extracted from DEG analysis and submitted as input to inquire a list of the chemical perturbagens altering the gene expression from iLINCS portal (<http://www.ilincs.org/ilincs/>). The discordant perturbagens with concordance score < -0.321 and the concordant perturbagens with concordance score > 0.321 were retained. Chemical perturbagens were clustered by mechanism of action (MOA) categories inquired from L1000 fireworks database, DrugBank database, and the Broad Institute database. The scripts for the analyses are available at https://github.com/willgryan/3PodR_bookdown and <https://github.com/CogDisResLab/BioPathNet>.

Immunofluorescence staining

IVC thrombi were harvested 48-hour post-stenosis, detached from the vessel wall, dried and weighed in a microbalance followed by embedded in optimal cutting temperature compound, frozen at -80°C , and was cut with a cryotome (CryoStar NX70 Cryostat; ThermoFisher Scientific) into 10- μm sections. 10 μm cryosections were then blocked in a ready-to-use protein block

(#ab64226, Abcam) for 30 min at room temperature followed by three times washing with 1X PBS-Tween (PBST). Sections were incubated overnight with primary antibodies for anti-rabbit Cit-Histone H3 (Arg2, Arg8, Arg17) (Thermo Fisher Scientific, #630-180ABBOMAX, 1:300) and FITC-Ly6G (Thermo Fisher Scientific, 11-9668-82, 1:250) at 4°C overnight. Next day, for anti-rabbit Cit-Histone H3 staining only, sections were washed with 1X PBST thrice and incubated with Alexa Fluor 647 goat anti-mouse (Thermo Fisher Scientific, #A21244, 1:500) secondary antibody for 1 h in the dark at room temperature. Slides were then washed three times with 1X PBST. All slides were then blotted dry, sealed with mounting medium containing DAPI (Thermo Fisher Scientific, #P36983) and allowed to dry overnight before imaging. Images were acquired using a fluorescence microscope EVOS™ M5000 Imaging System (Invitrogen) at 20 x magnification. Quantification was carried out using ImageJ software (NIH Image J, USA) and assessed with GraphPad Prism 8.0.0 to identify statistically significant differences among groups.

Flow-Cytometry

Blood samples (35µL) was collected into 25uL of dilute heparin (20U/mL in saline) and incubated with Fc block (1:15; Invitrogen, #14-0161-85) for 10min. Blood was then diluted 1:4 in PBS and incubated with the following antibodies for 20min at RT: 1:50 FITC anti-mouse CD45.2 (leukocytes; Biolegend #109806), 1:100 APC anti-mouse CD41 (platelets; Invitrogen #17-0411-82; 1:100), 1:100 BV650 anti-mouse Ter119 (red blood cells; #Biolegend 116235), 1:50 PE anti-mouse Ly-6G (neutrophils; BD Biosciences #551461), and 1:50 PE Cy7 anti-mouse CD115 (monocytes; Biolegend #135524). Zombie Violet was used elimination of dead leukocytes; Biolegend #423113; 1:200). Flow cytometry analysis was conducted on a 4 laser Acea NovoCyte Quanteon. Each sample had a stop condition of 1.2 million Ter119 positive events, with the flow rate set to 14µL/min. The threshold was lowered to 10,000 to visualize the small nature of platelets. Data analysis was performed using NovoExpress software. CBCs were analyzed using a Genesis automated hematology analyzer from Oxford Science.

Neutrophil static adhesion to VCAM-1

The coverslips were coated with 20 µg/ml recombinant mouse VCAM-1/CD106 Fc chimera protein (R&D Systems, Minneapolis, MN, #643-VM) by incubating it at 4°C overnight. The primary mouse bone marrow neutrophils were pretreated at different concentrations (0.01µM,

0.1 μ M 1 μ M, 10 μ M) of macitentan (Cayman Chemical, #23304) followed by its stimulation by TNF- α (20 ng/ml), and applied to the coverslip, and incubated for 30 mins at 37°C. The coverslips were washed with 1X PBS to remove non-adherent cells, and the attached cells were fixed and stained with Hoechst 33342 (Invitrogen, # R37605) and mounted on the slides. The number of adherent cells was counted in six random fields per coverslip. The images were captured at 20X magnification by EVOS™ M5000 Imaging System (Invitrogen) and counted by its built-in automated cell counter.

Neutrophil adhesion assay under flow

Flow chamber μ -slide VI 0.4 leuR ibiTreat (Ibidi) were coated with recombinant mouse VCAM-1/CD106 Fc chimera protein (R&D Systems, Minneapolis, MN, #643-VM) by incubating at 4°C overnight or by C57BL/6 Mouse Primary Vein Endothelial Cells (1×10^5) (Cell biologics, #C57-6009). Primary mouse bone marrow neutrophils from $\alpha 9^{fl/fl}$ and $\alpha 9^{fl/fl}Mrp8Cre^{+/-}$ mice or neutrophils pretreated with macitentan (1 μ M) and vehicle were stimulated by TNF- α (20 ng/ml) for 30 mins and labelled with Calcein, AM (5 μ M, Invitrogen) for 20 mins. The labelled neutrophils (1×10^5 /ml) were perfused under venous shear of 1 dyne/cm² for 5 mins over coated chamber slide using ibidi Pump System. Then the medium was perfused for an additional 3 mins to remove loosely bound cells. Images were recorded using EVOS™ M5000 Imaging System (Invitrogen) at 20X magnification. The adhered neutrophils were counted in different regions by a built-in automated counter in three independent experiments.

TUNEL assay

Bone marrow neutrophils from $\alpha 9^{fl/fl}$ and $\alpha 9^{fl/fl}Mrp8Cre^{+/-}$ mice were stimulated by 20 μ g/ml soluble Recombinant Mouse VCAM-1/CD106 Fc Chimera Protein (R&D Systems, Minneapolis, MN, #643-VM) and 20 ng/ml TNF- α (R&D Systems, Minneapolis, MN, #410-MT-010/CF) for 16-hrs. Then, C57BL/6 mouse primary vein endothelial cells (1×10^5) (Cell Biologics, #C57-6009) were treated with the supernatant of stimulated neutrophils for 6-hrs. Apoptosis of endothelial cells was measured with TUNEL staining using the Click-iT Plus TUNEL Assay In Situ Apoptosis Detection (Invitrogen, #C10618) using manufacturer's protocol. Briefly, cells were washed three times with 1X PBS followed by 4% paraformaldehyde (TissuePro technology, #PFA04-500R) fixation for 10 minutes at room temperature. After fixation cells were permeabilized with 0.25% Triton X-100 (Thermo scientific, #85111) for 20 minutes at room temperature followed by washing thrice with PBS. The cells are then processed for TUNEL staining according to manufacturer's

protocol and subsequently counter stained with DAPI. Images were observed and captured using EVOS™ M5000 Imaging System (Invitrogen) at 20X magnification. The number of apoptotic cells were quantified by counting TUNEL-positive cells in three independent experiments. Quantification was carried out using ImageJ software (NIH ImageJ, USA) and analyzed with GraphPad Prism 9.4.1 to identify statistically significant differences among groups.

Anti-VCAM-1 antibody administration

Mice were injected intravenously (30-min before surgery and 6-hr post-surgery) with purified NA/LE Rat Anti-Mouse VCA-1 (CD106; 100 µg/mouse, Clone 429 BD # 553329) or 100 µg Ultra-LEAF™ Purified Rat IgG1, κ Isotype Ctrl Antibody (BioLegend # 400431).

Ligand Preparation

The two-dimensional (2D) structure of Food and Drug Administration (FDA) approved drugs were retrieved from Selleckchem database, followed by the removal of ions, small fragments (< 250 dalton) and large molecules. In the final list, the 2D structure was standardized by salt removal and converted to 3D structure by OpenBabel version 2.3.2.

Homology modelling

The homology modeling was performed using the crystal structure of $\alpha 4\beta 1$ (PDB code: 3V4P) as a template in Swiss-Model online software to model $\alpha 9$ subunit (**supplemental Figure 23**). The aligned model was superimposed on $\alpha 4\beta 1$ and the coordinates of $\beta 1$ along with divalent ions Ca^{2+} and Mg^{2+} were extracted and merged with $\alpha 9$ subunit to make a full complex of $\alpha 9\beta 1$. The final model was thoroughly optimized to remove the steric clashes and validated using Ramchandran plot analysis.

Molecular docking

The molecular docking was performed by utilizing Autodock Vina with the PyRx interface tool. The 3D structures of the ligands and modelled protein were imported to PyRx and converted to pdbqt format. In the case of ligands, energy minimization was carried out using UFF force field methods before pdbqt conversion. The prepared ligands were docked in the complex with a grid considering the whole complex as a binding site in PyRx virtual screening tool using autodock Vina. The constraints were applied to metal ions and residue SER132, TYR133, SER144 and ARG243. The results were analyzed using maestro academic version 12.0.012.

Macitentan treatment

Macitentan was administered to WT mice as oral suspension in 0.25% N-methylpyrrolidone (Sigma # 328634), 0.25% Kolliphor HS 15 (Sigma # 42966) in sterile PBS at the dose of 5 mg/kg.

Statistical analysis

For analysis, GraphPad Prism software (9.4.1) was used. The Shapiro-Wilk test was used to check normality, and Bartlett's test was used to check equal variance. The results were considered significant at $P < 0.05$. Normally distributed data were analyzed by Student's t-test or Kruskal-Wallis test followed by corrected method of Benjamini and Yekutieli. Non-normally distributed data were analyzed using the Mann Whitney test. Thrombosis incidence data were analyzed using the Fisher's exact test. For RNA-seq data, Benjamini-Hochberg correction was used to obtain adjusted P-values. For all the in vivo experiments, we used a block randomization method in which an equal number of mice from each group were randomly selected to perform surgery on any given day. Sample size calculations: To detect a difference of 6 mg in thrombus weight with a standard deviation of 6.5, at overall significance levels of 0.05 with the power of 80%, 19 mice in each group will be required. To account for unexpected mortality following surgery, we performed surgery using $N=20$ in each group. Only mice that exhibited thrombosis were included to quantify the thrombus weight.

Table 1

Gene	Log2 Fold Change	
	WT Stimulated vs Unstimulated	Stimulated $\alpha 9^{fl/fl}$ Mrp8Cre ^{+/-} vs $\alpha 9^{fl/fl}$
Spp1	3.35	-4.32
Cxcl2	6.39	-4.63
Ccl3	7.69	-4.11
1700017B05Rik	1.84	-4.14
Maff	5.22	-4.98
Rhov	4.00	-5.67
Acod1	4.50	-1.92
Ccl4	5.46	-4.82
Plk3	4.06	-4.57
Tnfrsf26	5.05	-3.54
Nlrp3	6.32	-2.54
Arl5b	3.88	-2.90
Dusp5	4.45	-2.83
Csrnp1	4.09	-2.67
Plau	2.93	-3.85
Lilrb4a	7.66	-3.15
4833407H14Rik	1.66	-4.42
Hmmr	-0.27	3.99
Rgs1	0.78	-4.92
Ier3	4.05	-1.90
Epb42	-2.25	4.30
Moap1	3.86	-3.88
Cd200r4	4.35	-4.80
Olr1	6.56	-2.70
E230013L22Rik	3.91	-5.38
P2ry2	4.57	-2.74
Kctd11	0.77	-4.30
Ggta1	4.04	-3.31
Fosl1	4.37	-3.03
Eaf1	5.09	-1.80
Cd79a	-1.24	4.81
Lamb3	2.44	-4.73
Castor1	2.39	-4.75
Slc35d2	0.90	-4.18
Clspn	-0.99	3.92
Aim2	1.23	-3.98
1600010M07Rik	-1.28	-4.03
Galnt3	-1.75	-4.06
Cnr2	0.09	-4.03
Tal1	-1.03	5.30
Morrbid	2.38	-4.42
Pdcd1lg2	1.37	-5.54
Rnaseh2b	-2.98	4.59
H2ac18	2.42	-4.35
Tlr6	3.07	-5.03

Slc51a	0.27	-4.77
S1pr2	4.55	-3.00
Trem14	3.46	4.57
Zc3h12a	0.36	-3.93
Mns1	-4.17	3.22
Apol11b	-1.98	5.39
Tnfsf14	0.40	-3.95
Gfi1b	-0.42	3.92
Bmf	0.49	3.94
Dnase111	-0.98	4.26
Cd80	0.17	-4.10
Gm17344	-0.46	-3.89
2310039H08Rik	-0.96	3.98
Ldhc	-4.27	-3.41
Prok2	0.31	-4.83
Ppp1r13l	4.29	-3.39
Il1a	3.10	-4.19
Egr2	4.04	-2.39
E230032D23Rik	0.56	-4.24
Chaf1b	4.26	-2.66
Bcl2a1d	5.66	2.44
Tspan8	-0.10	5.12
Gypc	-1.64	4.15
F13a1	-4.49	1.54
Spib	-2.86	4.31
Bcl2a1b	3.92	-1.20
Nr4a3	4.60	-1.44
Rad51	0.30	3.91
Upp1	5.09	-0.65
Nfkbiz	4.03	-0.94
Bmx	-4.46	2.07
Sfn14	-5.35	1.28
Trim58	-4.07	0.68
Stab2	-4.88	-0.77
Cd200r1	4.06	-1.14
Inka1	-4.45	-0.23
Hoxc10	-5.01	-0.45
Ifnlr1	4.00	0.11
Dapk2	-4.14	1.12
Wdr86	-4.49	0.15
Fcgr4	-4.39	0.63
Jaml	-5.02	0.62
Bcl2a1a	4.08	0.24
Gm15441	4.34	-0.23
Kif4	-4.24	-0.07
Metrn1	5.56	-0.27
Nfkbib	4.72	-0.06

Table 2

Gene	Sense	Antisense
<i>Gapdh</i>	GGGTGTGAACCACGAGAAATA	CTGTGGTCATGAGCCCTTC
<i>Actb</i>	GGCTGTATTCCCCTCCATCG	CCAGTTGGTAACAATGCCATGT
<i>Itga9</i>	TGCTTTCCAGTGTTGACGAGA	TTAAAGGACACGTTGGCATCATA
<i>Bcl-2</i>	GCTACCGTCGTGACTTCGC	CCCCACCGAACTCAAAGAAGG
<i>Caspase3</i>	CTGACTGGAAAGCCGAAACTC	CGACCCGTCCTTTGAATTTCT
<i>P-Selectin</i>	CCCTGGCAACAGCCTTCAG	GGGTCCTCAAATCGTCATCC
<i>E-Selectin</i>	ATGAAGCCAGTGCATACTGTC	CGGTGAATGTTTCAGATTGGAGT
<i>Icam-1</i>	CAGGAGGAGGCCATAAACTC	TCTGTGACAGCCAGAGGAAGT
<i>Vcam-1</i>	ATTGGGAGAGACAAAGCAGAAG	CTCCAAGAAAAGAAGGGGAGT
<i>Il-6</i>	CTGCAAGAGACTTCCATCCAG	AGTGGTATAGACAGGTCTGTTGG
<i>Nlrp3</i>	ATCAACAGGCGAGACCTCTG	GCCTCCTGGCATAACCATAGA

Table Legends:

Table 1: List of shared DEGs and their log₂ fold change from RNA-seq data of neutrophils isolated from WT mice and stimulated neutrophils isolated from neutrophil-specific $\alpha 9^{-/-}$ mice and littermate controls.

Table 2: List of primer sequences.

Figure Legends:

Supplemental Figure 1: Demographical and clinical characteristics of patients with stroke.

Supplemental Figure 2: Male WT mice were subjected to embolic stroke or sham surgery. Plasma and IVC samples were isolated 6-hr post stroke. (A) Plasma levels of PAI-1 (U/L; plasminogen activator inhibitor-1). (B) Plasma levels of TAT (pg/mL; thrombin antithrombin complex). (C) Plasma levels of fibrinogen ($\mu\text{g/mL}$). IVC samples were used to prepare RNA and cDNA. qRT-PCR analysis of *Vcam1* (D), *seip* (E), *Sele* (F), and *Icam1* (G) relative to *Actb*. Data are mean \pm SEM and analyzed by the Mann Whitney test; n = 4-5.

Supplemental Figure 3: (A). Breeding strategy used to generate neutrophil-specific $\alpha 9^{-/-}$ mice. (B) Representative genomic PCR images confirming MRP8Cre gene. (C) Western blot images of integrin $\alpha 9$ from the neutrophils isolated from neutrophil-specific $\alpha 9^{-/-}$ mice and littermate controls. (D) Tail bleeding time. (E) Blood neutrophil count. Data are mean \pm SEM and analyzed by an unpaired Student t test; n = 6 (D-E).

Supplemental Figure 4: (A) Left, representative cross-sectional immunofluorescence image of the isolated IVC thrombus (48-hour post-stenosis) from each group for TUNEL (red) and DAPI (blue). Magnification 20X; Scale bar 50 μm . Right, quantification. (B) Representative cross-sectional immunofluorescence image of the isolated IVC thrombus (48-hour post-stenosis) from each group for the monocytes (Ly6C) (green) and DAPI (blue). Magnification 20X; Scale bar 50 μm . Right, quantification. Data are mean \pm SEM and analyzed by the Mann Whitney test; n = 7.

Supplemental Figure 5: (A) Representative gating strategy used to detect % platelet-neutrophils and %platelet-monocytes aggregates 6-hr after stroke-DVT surgery. (B) Quantification for % platelet-neutrophils aggregates. (C) Quantification for % platelet-monocytes aggregates. Data are mean \pm SEM and analyzed by the Mann Whitney test; n = 5.

Supplemental Figure 6: Littermate controls and neutrophil specific integrin $\alpha 9^{-/-}$ mice were subjected to IVC stasis. (A) Representative IVC thrombus harvested 48-hour post-stasis from each group. Right, thrombus weight (mg). Only mice that exhibited thrombosis were included to quantify the thrombus weight. Each dot represents a single mouse. Data are mean \pm SEM and analyzed using the Mann Whitney test (A), Fisher's exact test (B); n=12

Supplemental Figure 7: Mice were subjected to IVC stenosis. IVC thrombus weight 48-hour post-stenosis in each group. Data are mean \pm SEM and analyzed by the Mann Whitney test; n = 9.

Supplemental Figure 8: WT neutrophils were stimulated with VCAM-1 (10 μ g/mL), or TNF- α (20 ng/mL) or VCAM-1 (10 μ g/mL) + TNF- α (20 ng/mL). cFDNA and elastase in cell supernatant were analyzed at 6-hr post stimulation. Data are mean \pm SEM and analyzed using the Kruskal-Wallis test followed by corrected method of Benjamini and Yekutieli ; n=3.

Supplemental Figure 9: (A) Hierarchical clustering of gene expression revealed gene clusters that were significantly changed in stimulated and unstimulated neutrophils of WT mice. (6-hour post-stimulation with VCAM-1 and TNF-alpha). (B) Hierarchical clustering of gene expression revealed gene clusters that were significantly changed in stimulated neutrophils of neutrophil-specific $\alpha 9^{-/-}$ mice and littermate controls.

Supplemental Figure 10: (A) Normalized log₂ fold change of top-20 genes from RNA-seq data (6-hour post-stimulation with VCAM-1 and TNF-alpha) of neutrophils isolated from WT mice. (B) Normalized log₂ fold change of top-20 genes from RNA-seq data (6-hour post-stimulation with VCAM-1 and TNF-alpha) of neutrophils isolated from neutrophil-specific $\alpha 9^{-/-}$ mice and littermate controls.

Supplemental Figure 11: (A) GSEA was performed based on RNA-sequencing of stimulated and unstimulated WT neutrophils and (B) stimulated neutrophils from littermate controls and neutrophil specific integrin $\alpha 9^{-/-}$ mice. The significance of the enriched pathways was determined by right-tailed Fisher's exact test followed by Benjamini-Hochberg multiple testing adjustment, n = 5 (A), n = 4-5 (B).

Supplemental Figure 12: (A) Upregulated and down regulated GO biological processes from RNA-seq data (6-hour post-stimulation with VCAM-1 and TNF-alpha) of neutrophils isolated from WT mice. (B) Upregulated and down regulated GO biological processes from RNA-seq data (6-hour post-stimulation with VCAM-1 and TNF-alpha) of neutrophils isolated from neutrophil-specific $\alpha 9^{-/-}$ mice and littermate controls.

Supplemental Figure 13: (A) Left, representative western blot images of pERK and total ERK from the VCAM-1+TNF-alpha stimulated neutrophils of littermate controls and neutrophil-specific $\alpha 9^{-/-}$ mice and. Right, quantification. (B) Neutrophils were pretreated with 10 μ M U0160, followed

by stimulation with VCAM-1+TNF-alpha. Elastase was analyzed in cell-culture media 6-hr post-stimulation from the stimulated neutrophils of neutrophil-specific $\alpha 9^{-/-}$ mice and littermate controls. Data are mean \pm SEM and analyzed by the Mann Whitney test (A) or by Kruskal-Wallis test followed by Fisher's LSD test (B), n = 4 (A-B).

Supplemental Figure 14: qRT-PCR validation of selected apoptosis and inflammation related genes relative to *Gapdh* in mouse endothelial cells incubated with cell supernatant of stimulated neutrophils from $\alpha 9^{fl/fl}$ and $\alpha 9^{fl/fl}Mrp8Cre^{+/-}$ mice. Data are mean \pm SEM and analyzed by an unpaired Student t test, n=6.

Supplemental Figure 15: Mice were injected intravenously (30-min before surgery and 6-hr post-surgery) with purified NA/LE rat anti-mouse VCAM-1 (CD106; 100 μ g/mouse, Clone 429 BD # 553329) or 100 μ g Ultra-LEAF™ purified tat IgG1, κ isotype ctrl antibody (BioLegend # 400431). (A) Representative IVC thrombus harvested 48-hour post-stasis from each group. Right, thrombus weight (mg). Only mice that exhibited thrombosis were included to quantify the thrombus weight. Each dot represents a single mouse. Data are mean \pm SEM and analyzed using the Kruskal-Wallis test followed by corrected method of Benjamini and Yekutieli (A), Fisher's exact test (B); n=20

Supplemental Figure 16: Binding pose and binding energy for top hits with $\alpha 9\beta 1$.

Supplemental Figure 17: Binding pose and binding energy for macitentan with integrin $\alpha 4\beta 1$.

Supplemental Figure 18: Top, representative images of the human neutrophil adhesion to the HUVEC coated slides at venous shear rate Magnification 20X; Scale bar 50 μ m. Bottom, qualification. Data are mean \pm SEM and analyzed by an unpaired Student t test, n=6.

Supplemental Figure 19: Mice were administered orally with macitentan (2 mg/kg, daily once for 5 days) or equal amount of vehicle. (A) Representative IVC thrombus harvested 48-hour post-stasis from each group. Right, thrombus weight (mg). Only mice that exhibited thrombosis were included to quantify the thrombus weight. Each dot represents a single mouse. Data are mean \pm SEM and analyzed using the Mann Whitney test (A), Fisher's exact test (B); n=20.

Supplemental Figure 20: WT mice were treated with vehicle or macitentan for 5 days, followed by IVC stenosis. (A) Plasma elastase and (B) plasma MPO from at 48-hour post stenosis from each group. Data are mean \pm SEM and analyzed by an unpaired Student t test, n=10.

Supplemental Figure 21: Mice were administered orally with macitentan (5 mg/kg, daily once for 5 days) or equal amount of vehicle. Plasma and IVC samples were isolated 6-hr after the last dose and analyzed for VCAM-1 (ng/mL) (A), circulating neutrophils ($10^3/\mu\text{L}$) (B), circulating monocytes ($10^3/\mu\text{L}$) (C), circulating platelets ($10^3/\mu\text{L}$) (D), *Icam1* gene expression in IVC (E), *Seip* gene expression in IVC (F), *Sele* gene expression in IVC (G), plasma fibrinogen ($\mu\text{g/mL}$) (H), plasma TAT (pg/mL) (I), and plasma PAI-1 (U/L) (J). Data are mean \pm SEM and analyzed by the Mann Whitney test, n=5.

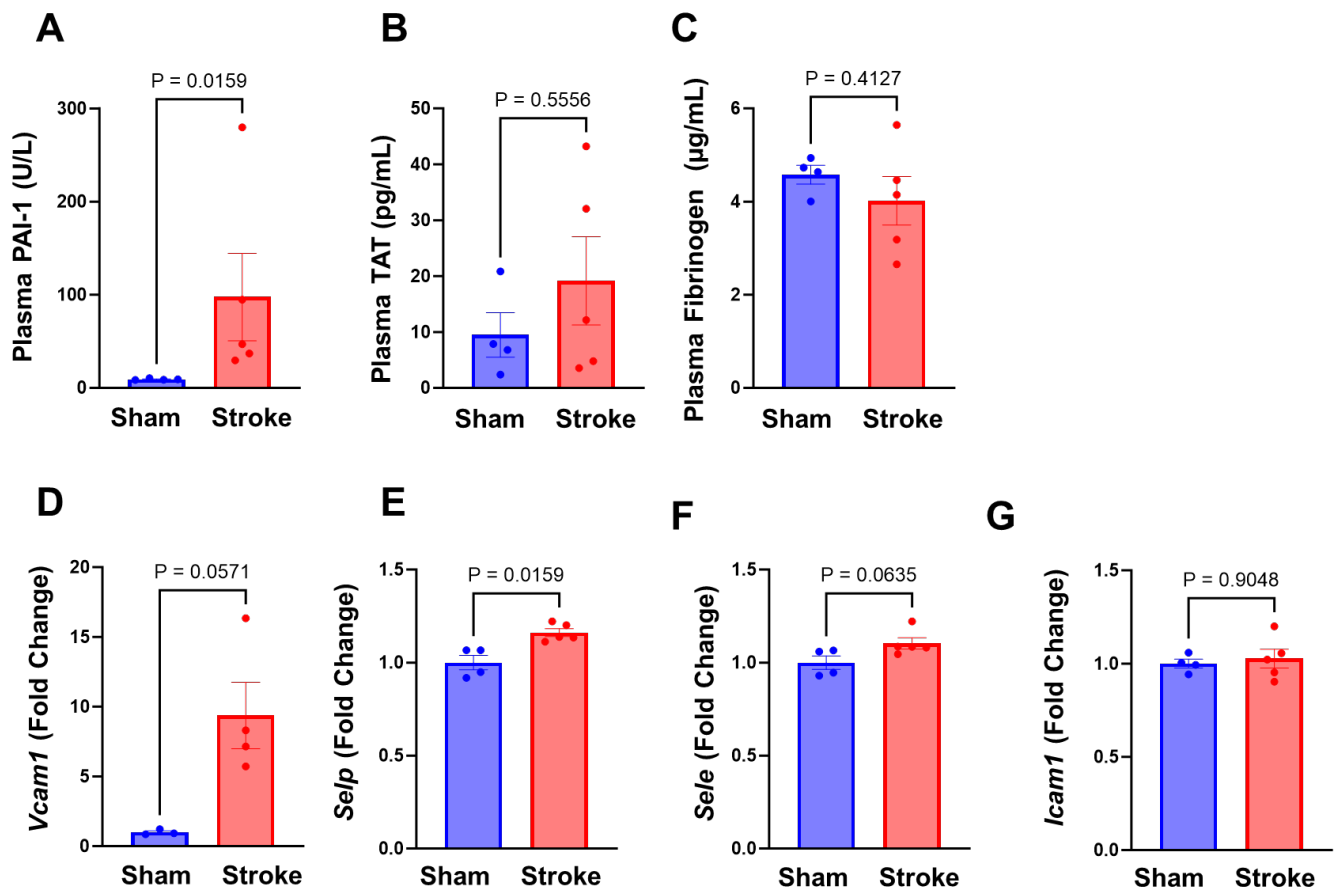
Supplemental Figure 22: Left, representative images of the neutrophil adhesion to the VCAM-1 coated slides at venous shear rate. Magnification 20X; Scale bar 50 μm . Right, qualification. Data are mean \pm SEM and analyzed by Kruskal-Wallis test followed by the corrected method of Benjamini and Yekutieli, n=6.

Supplemental Figure 23: Alignment of the amino acid sequences of integrin $\alpha 9$ and the crystal structure of integrin $\alpha 4$ (PDB code: 3V4P). 'I' represents positions that have single, fully conserved residue; ':' indicates conservation between groups of strongly similar properties; '.' indicates conservation between groups of weakly similar properties.

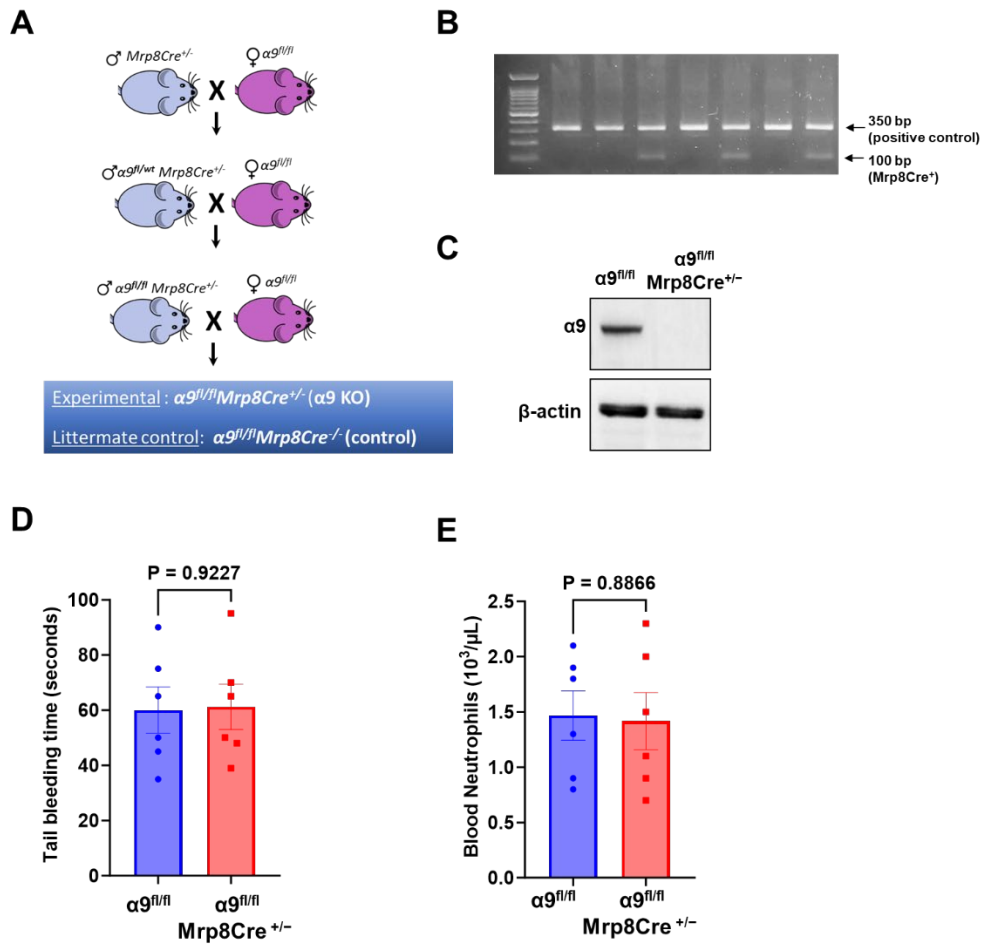
Supplemental Figure 1

No.	Age	Sex	Stroke etiology	Race	Occlusion site	Artery involvement	NIHSS at admission	Mechanical Thrombectomy	tPA
1	62	M	Intracranial	White	Left M2	Left MCA	6	Y	N
2	72	F	Cardiac	Black	Left M1	Left MCA	31	Y	Y
3	68	F	Carotid	Black	Left CCA	Left CCA	19	Y	N
4	59	F	Cardiac	White	left M1L	Left MCA	4	Y	Y
5	57	F	Intracranial	White	Left MCA	Left MCA	10	N	N
6	72	F	Intracranial	White	Left M1	Left MCA	17	Y	Y
7	82	F	Intracranial	Black	Right M2	Right MCA	8	N	N
8	46	F	Embolitic stroke of undetermined source	Black	Left M2	Left MCA	14	N	N

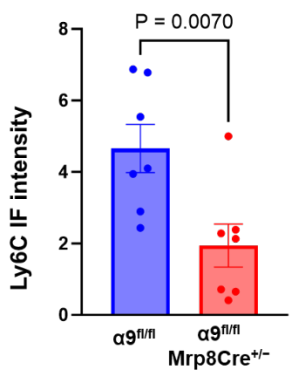
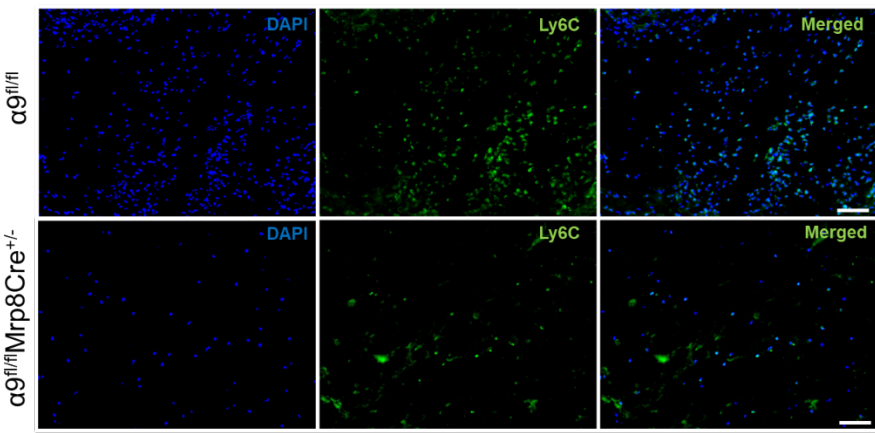
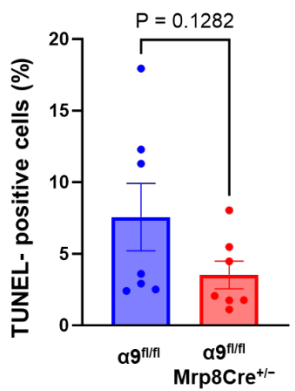
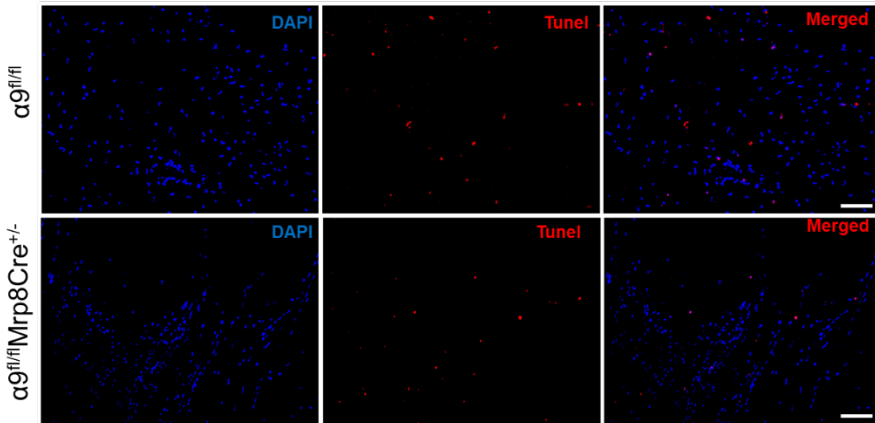
Supplemental Figure 2



Supplemental Figure 3

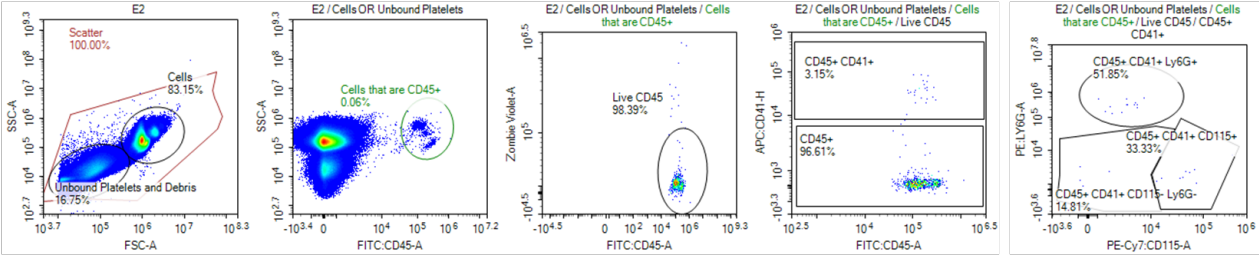


Supplemental Figure 4

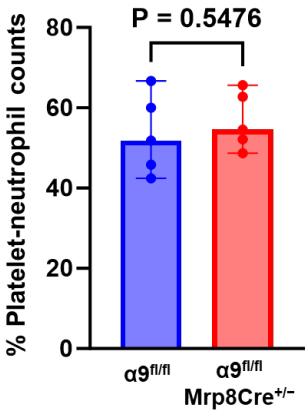


Supplemental Figure 5

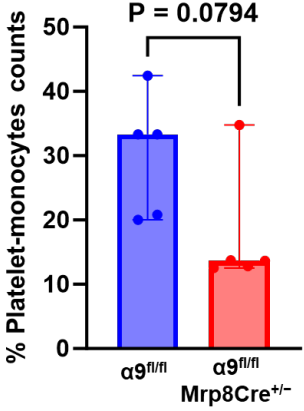
A



B

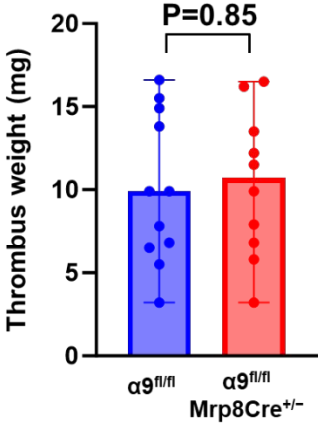
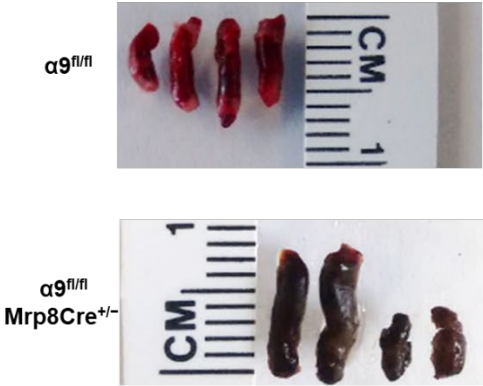


C

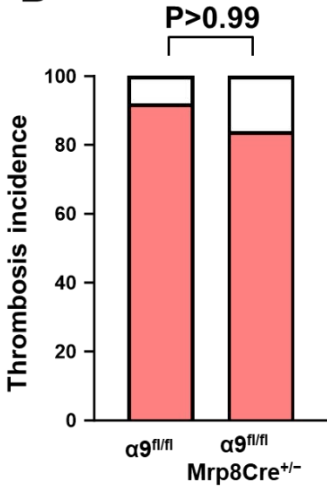


Supplemental Figure 6

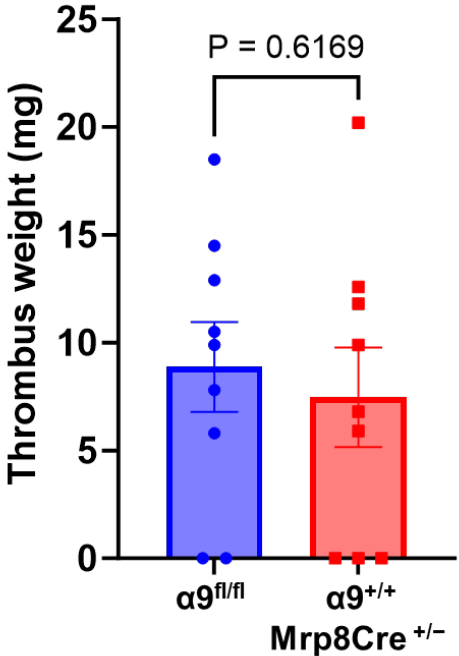
A



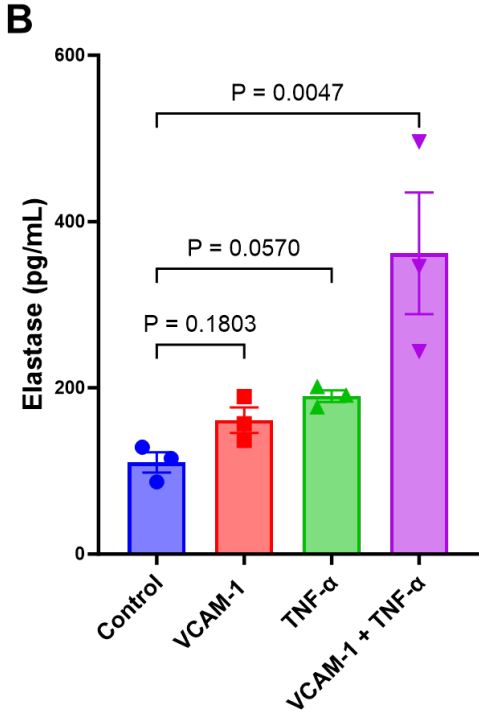
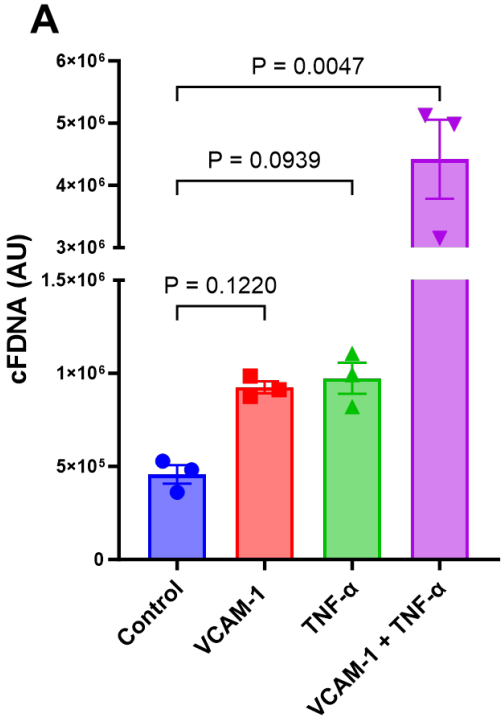
B



Supplemental Figure 7

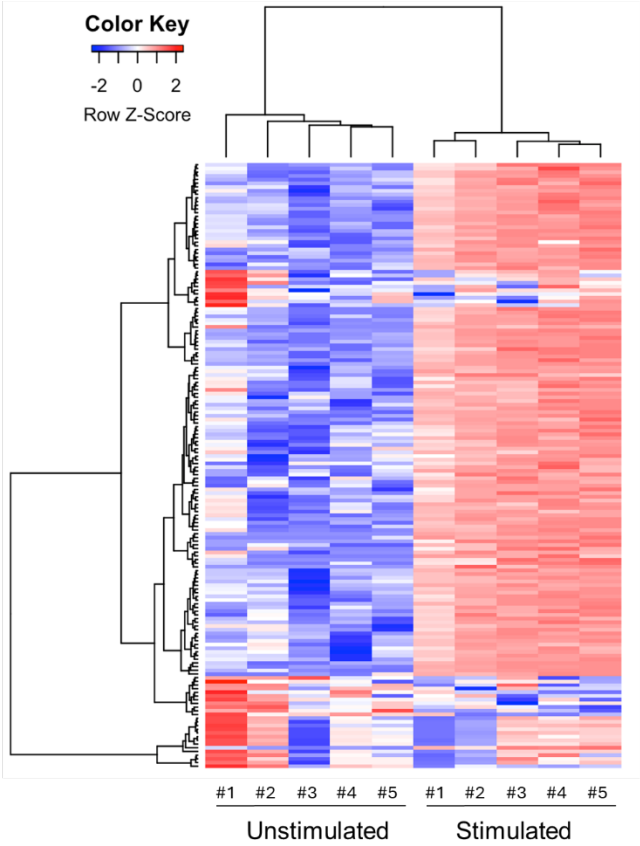


Supplemental Figure 8

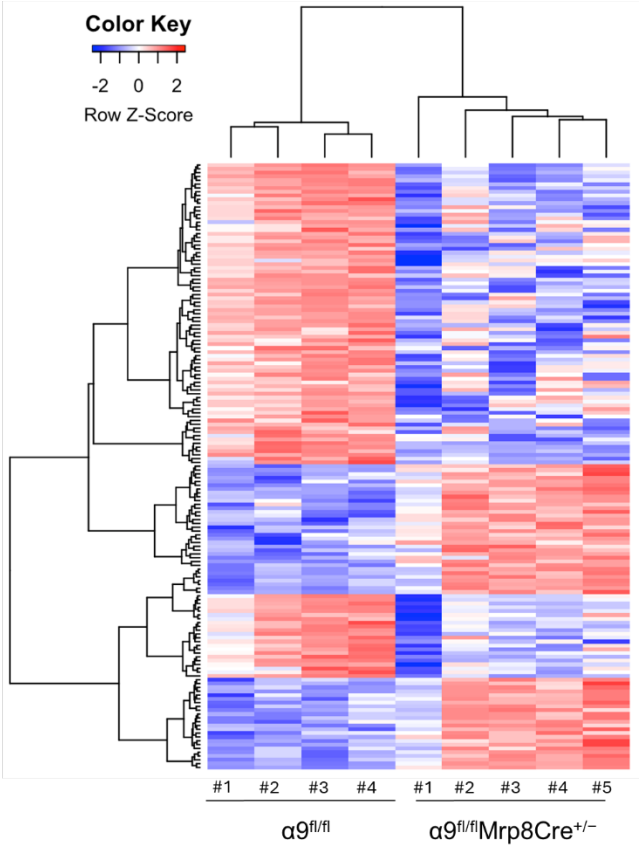


Supplemental Figure 9

A

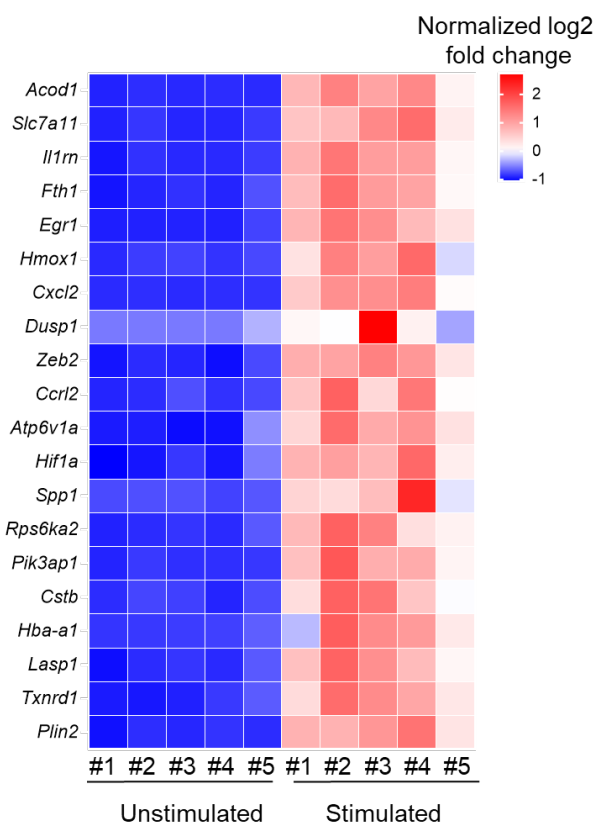


B

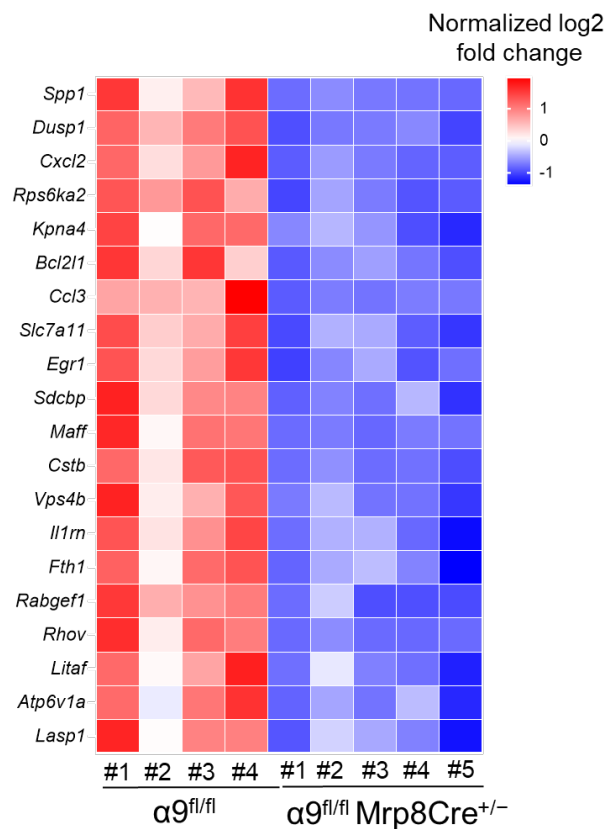


Supplemental Figure 10

A



B



Supplemental Figure 11

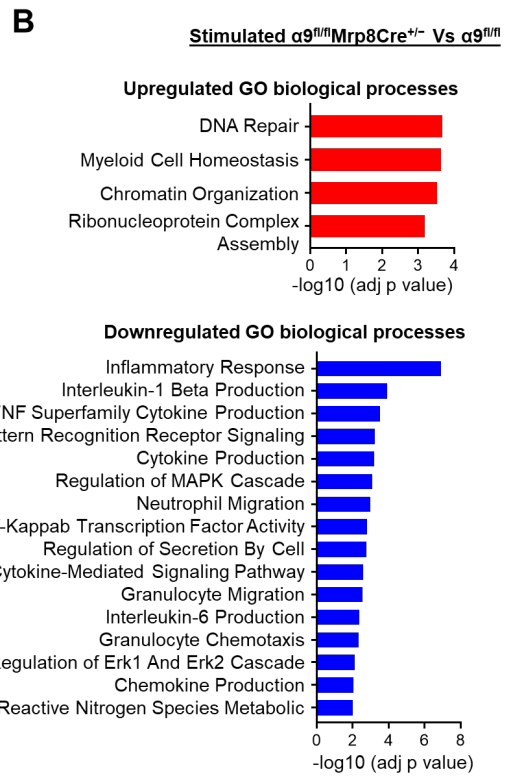
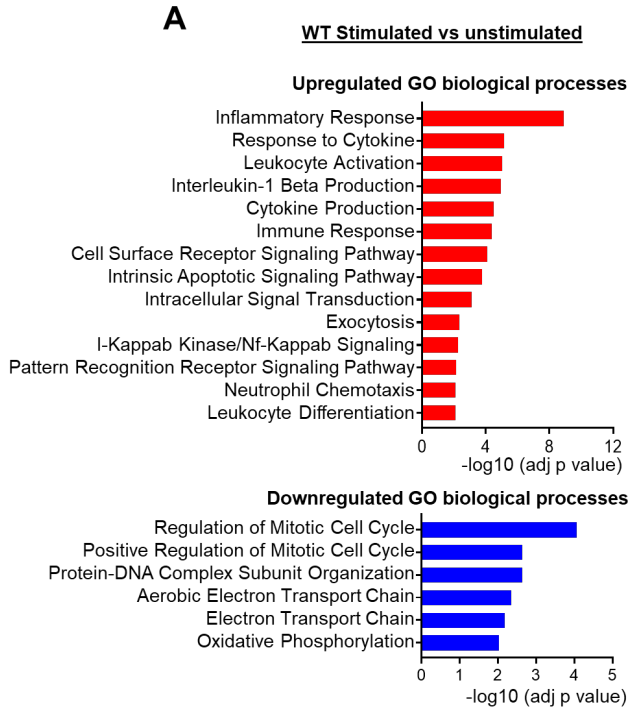
A

GO ID	Pathway	NES	Adj. P value
0006954	inflammatory response	2.65	1.20E-09
0050727	regulation of inflammatory response	2.48	4.68E-07
0007165	signal transduction	1.95	2.04E-06
0007154	cell communication	1.89	3.18E-06
0006952	defense response	2.14	4.00E-06
0023052	signaling	1.87	4.96E-06
0034097	response to cytokine	2.21	7.13E-06
0007166	cell surface receptor signaling pathway	2.06	9.13E-06
0035556	intracellular signal transduction	1.91	1.09E-05
0048583	regulation of response to stimulus	1.87	1.26E-05

B

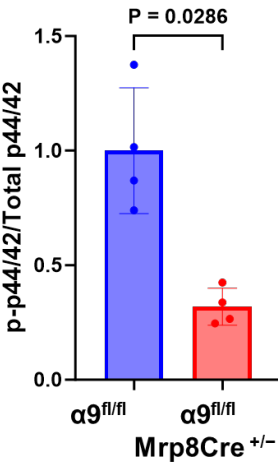
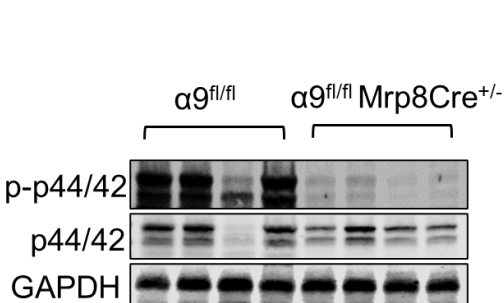
GO ID	Pathway	NES	Adj. P value
0006954	inflammatory response	-2.57	1.26E-07
0050727	regulation of inflammatory response	-2.59	1.96E-06
0022613	ribonucleoprotein complex biogenesis	2.82	1.97E-06
0030218	erythrocyte differentiation	2.85	3.01E-06
0034101	erythrocyte homeostasis	2.71	4.67E-06
0031347	regulation of defense response	-2.44	4.72E-06
0032101	regulation of response to external stimulus	-2.27	2.06E-05
0023052	signaling	-1.91	3.66E-05
0050729	positive regulation of inflammatory response	-2.30	4.06E-05
0048821	erythrocyte development	2.60	4.38E-05

Supplemental Figure 12

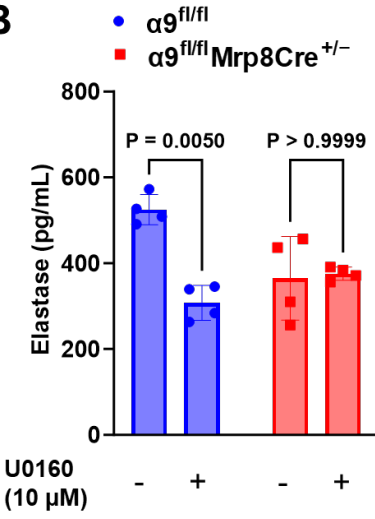


Supplemental Figure 13

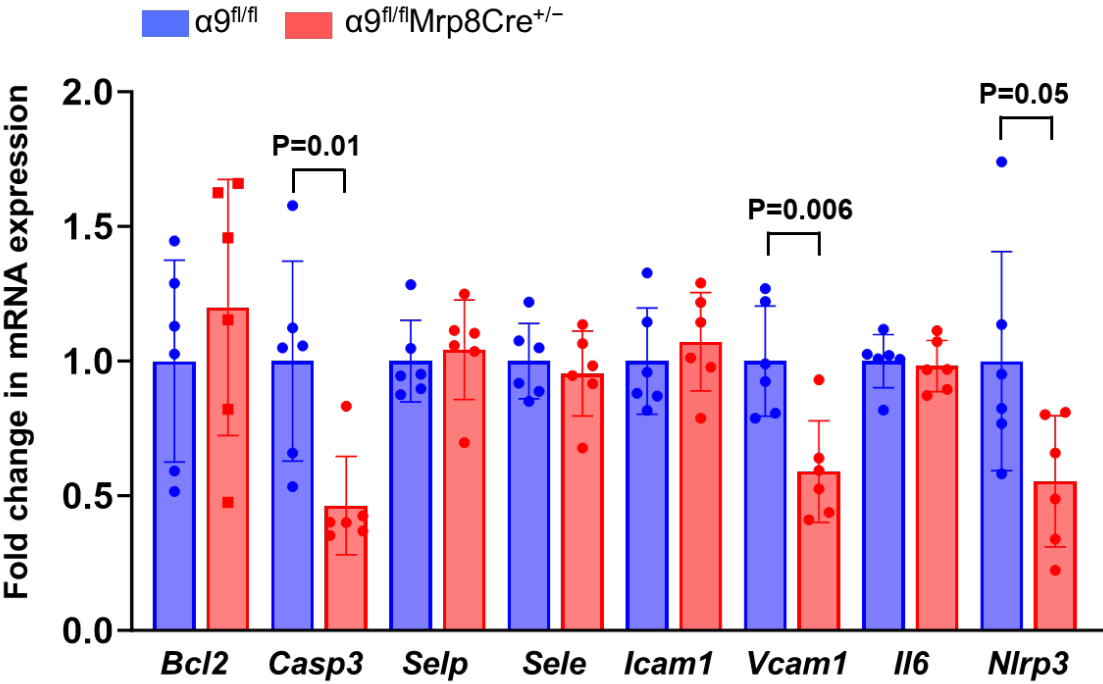
A



B

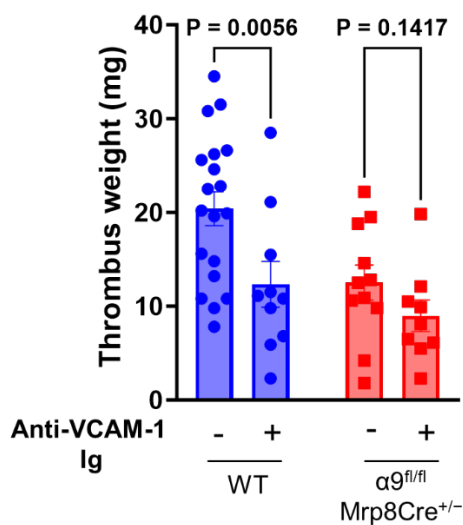
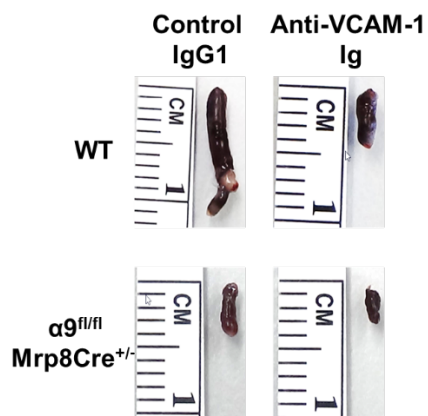


Supplemental Figure 14

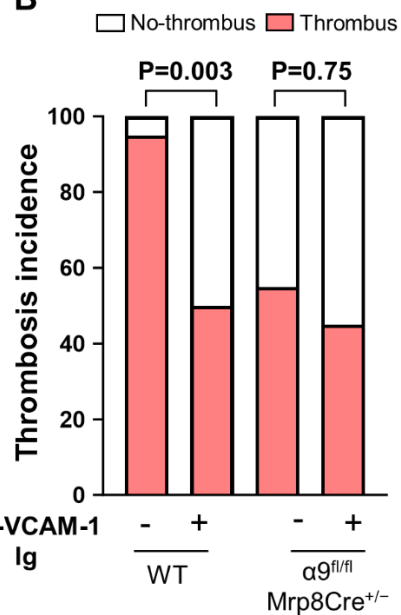


Supplemental Figure 15

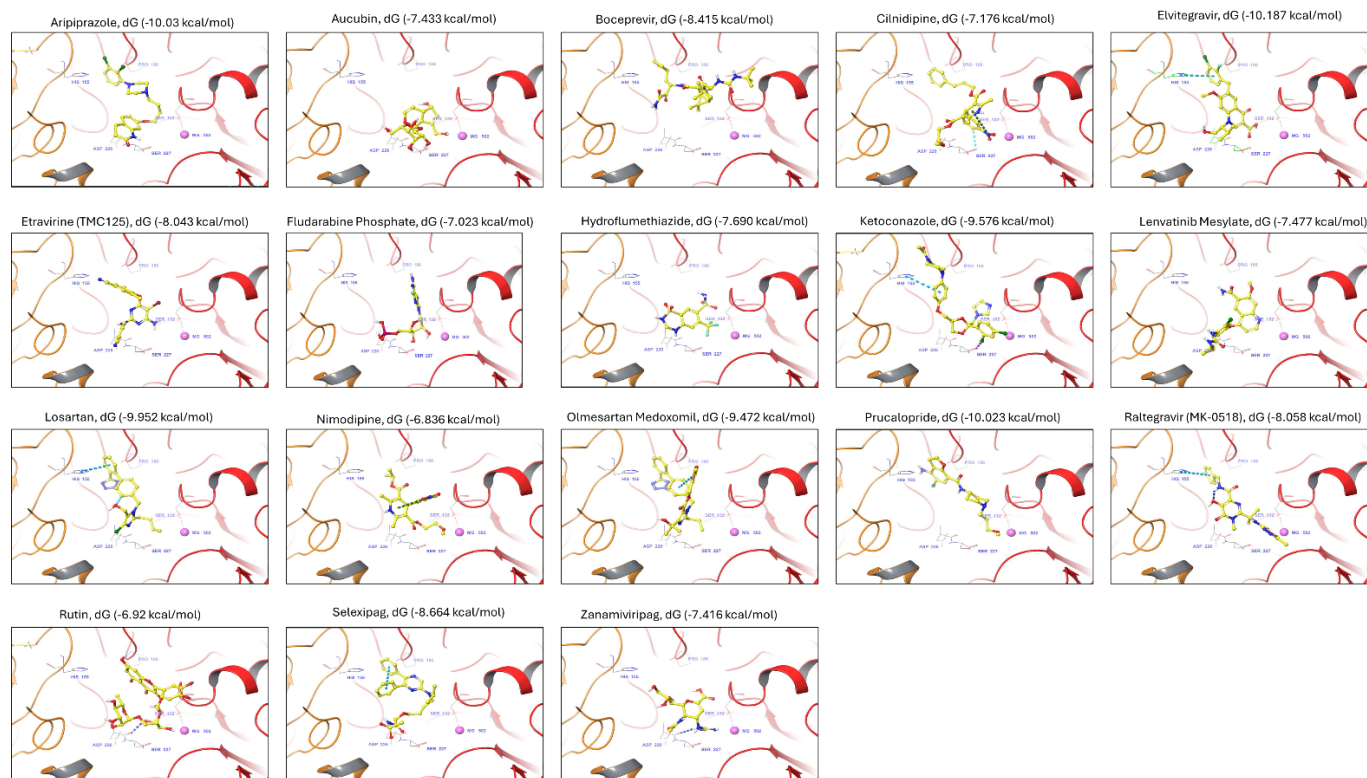
A



B

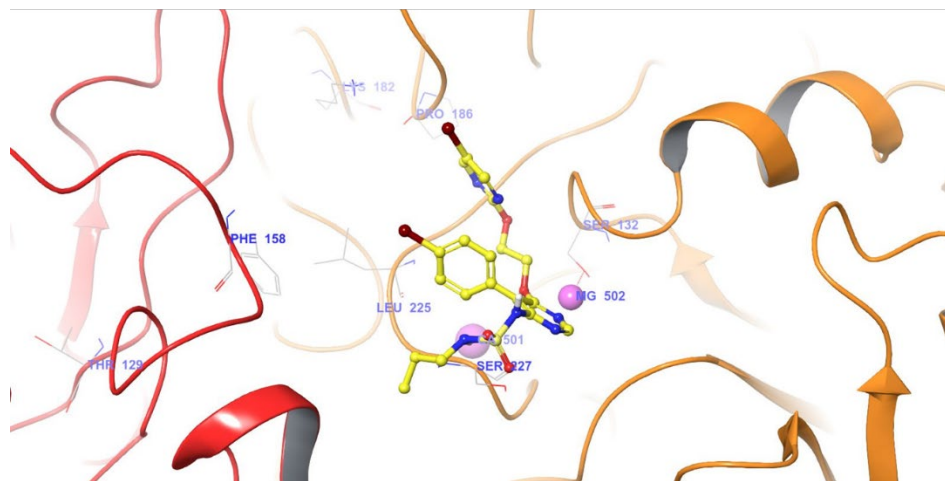


Supplemental Figure 16

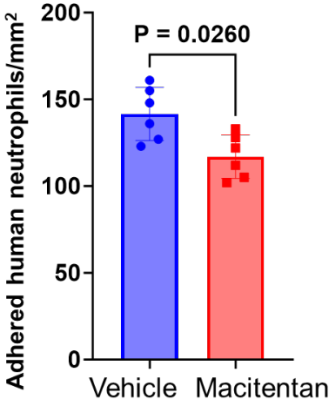
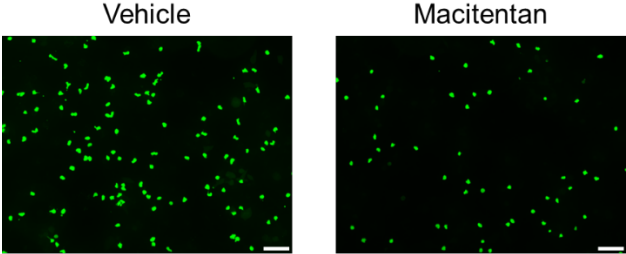


Supplemental Figure 17

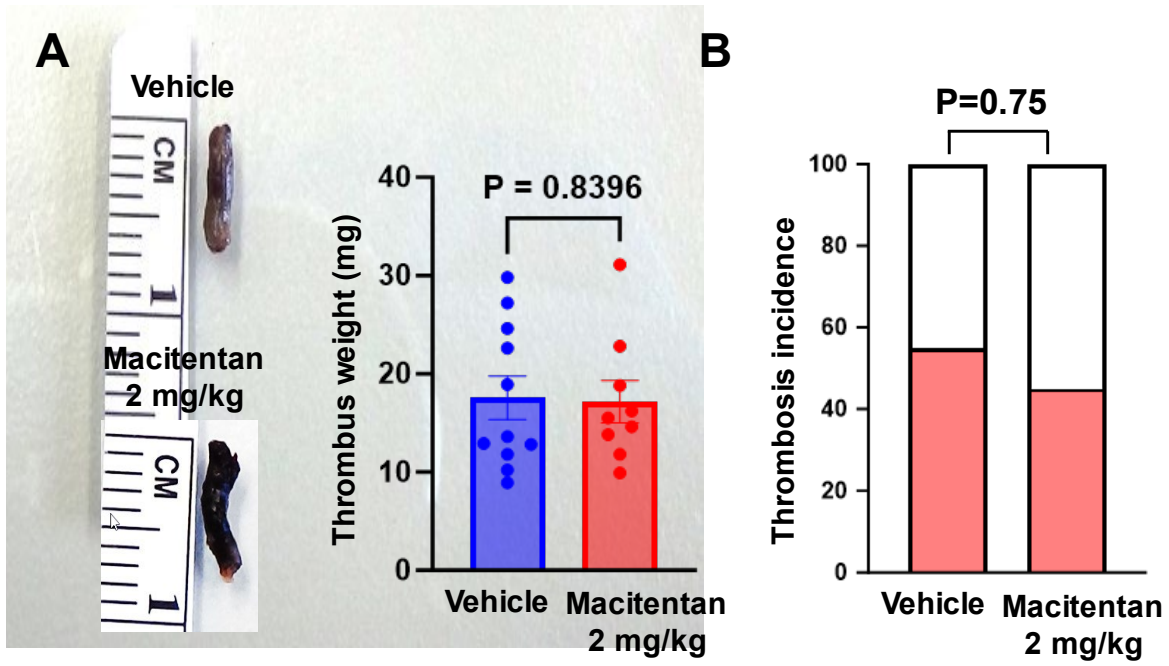
Macitentan with $\alpha\beta41$
Binding energy: -6.922 kcal/mol



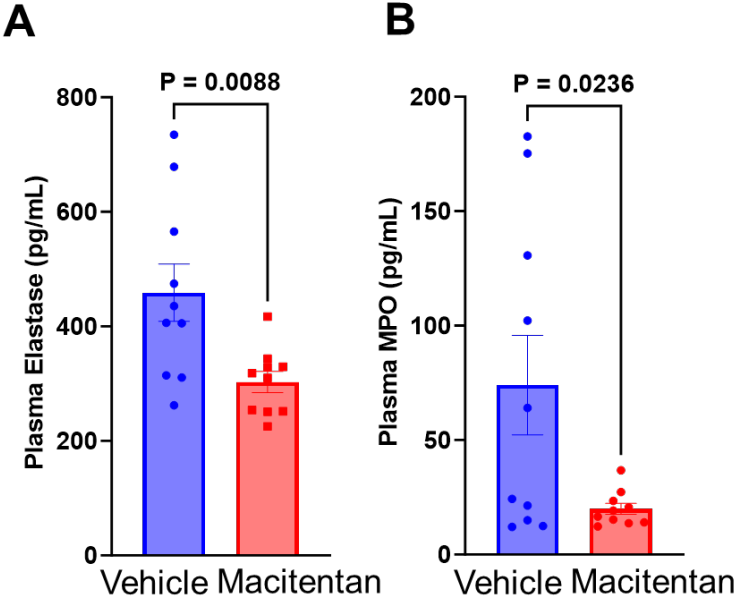
Supplemental Figure 18



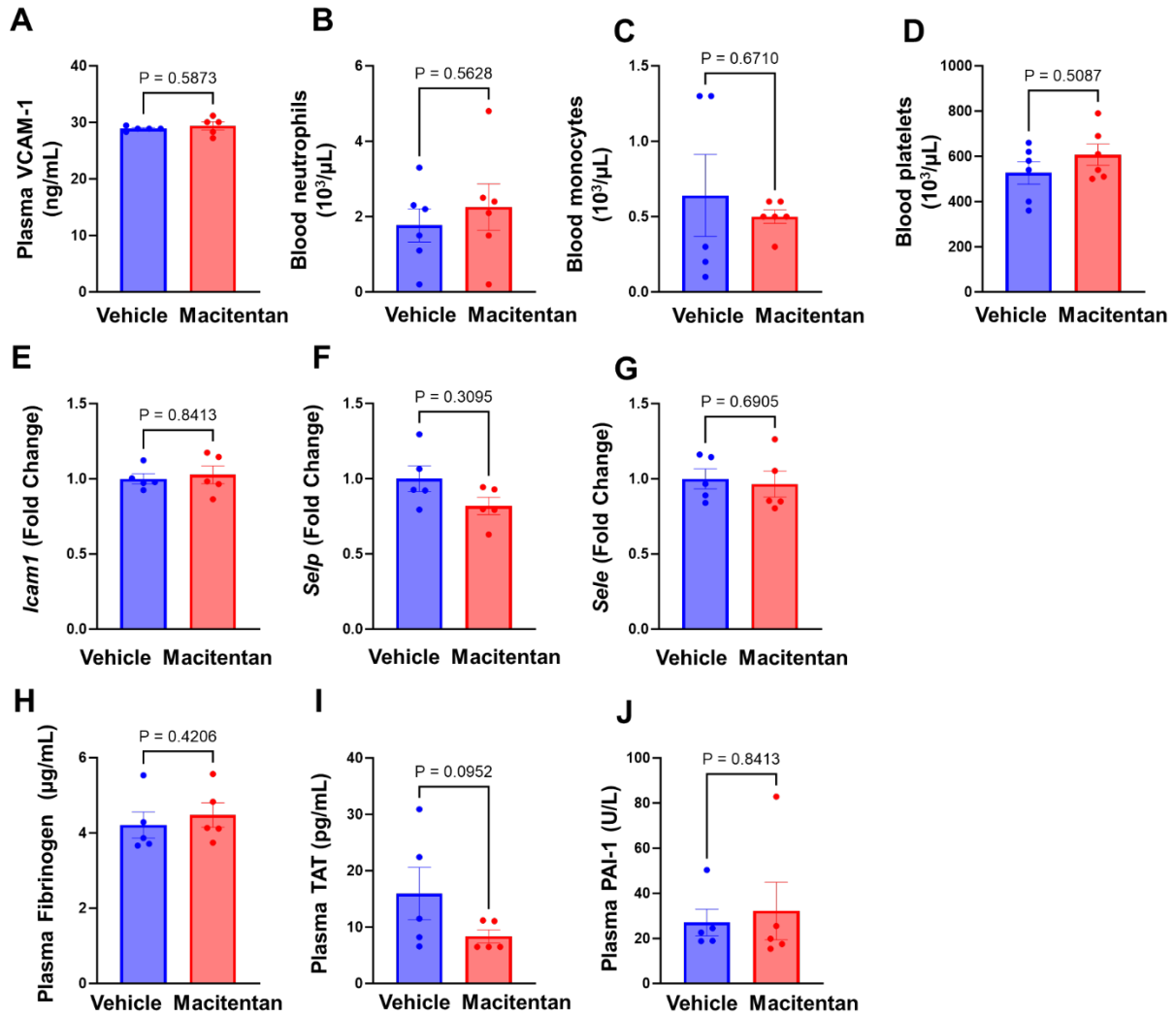
Supplemental Figure 19



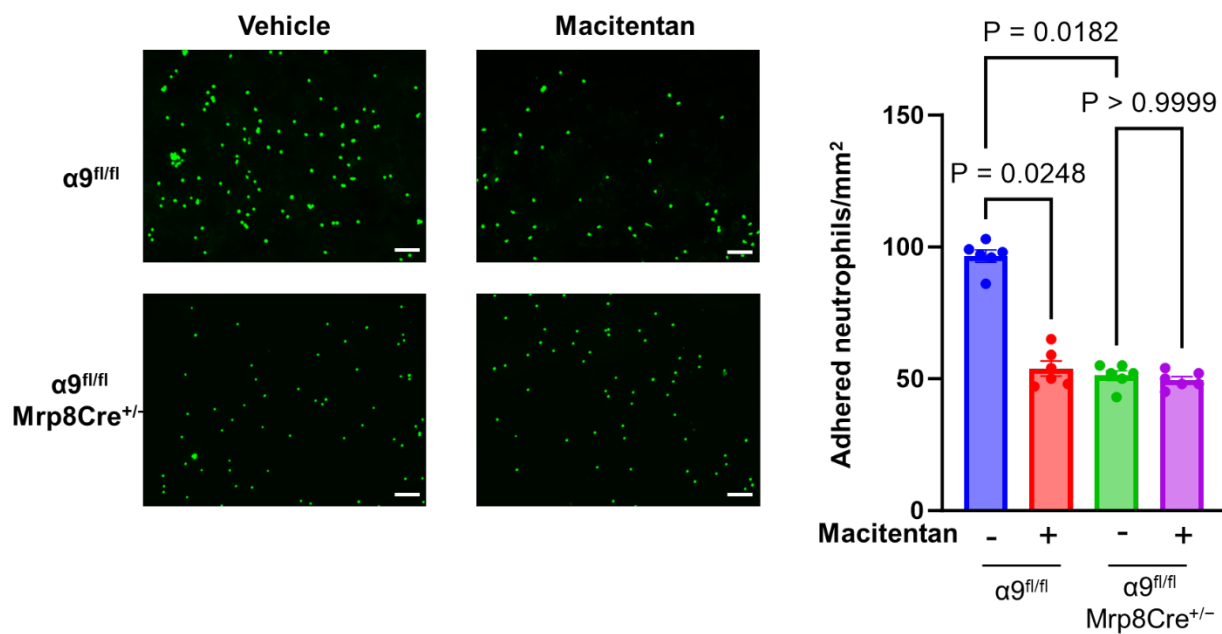
Supplemental Figure 20



Supplemental Figure 21



Supplemental Figure 22



Supplemental Figure 23

hITA4	1 MAWEARREPGPRRAA-VRETVMLLLCLGVPTGRPYNVDTESALLYQGFHN	49
hITA9	1 MGGPA---APRGAGRLRALLLALVVGIPAG-AYNLDPQRPVHFQGPAD	45
hITA4	50 TLFYGSVVLHSHGANRWLLVGAAPTANWLANASVINPGAIYRCRIGKNPGQ	99
hITA9	46 SFFGYAVLEHFHDNTRWVVLVGA PKADSKYSPSVKSPGAVFKCRVHTNPDR	95
hITA4	100 TCEQLQL--GSPNGEPCGKTCLEERDNQWLGVTLRQPGENGSIIVTCGHR	147
hITA9	96 RCTELDMARGKNRGTSCGKTCREDRDEWGMVSLARQPKADGRVLACAH	145
hITA4	148 WKNIFYIKENKLPSTGGCYGVPPDLRTELSKRIAPCYQDYVKKFGENFAS	197
hITA9	146 WKNIIYY-EADHILPHGFCYIIIPSNLQAK-GRTLIPCYEYKKKYGEEHGS	193
hITA4	198 CQAGISSFYTKDLIVMGAPGSSYWTGSLFVYNITTNKYKAFLDRKQNVKF	247
hITA9	194 CQAGIAGFFTEELVVMGAPGSFYWAGTIKVLNLDNTYLLKLNDEVIMNRR	243
hITA4	248 GSYLGYSVGAGHFERSQHTTEVVGAPQHEQIGKAYIFSIDEKE--LNILH	295
hITA9	244 YTYLGYAVTAGHFSPSTIDVVGAPQDKGIGKVIYFRADRRSGTLIKIF	293
hITA4	296 EMKGRKLGSYFGASVCAVDLNDGFSDDL VGAPMQSTIREEGRV FVYINS	345
hITA9	294 QASGKKMGSYFGSSLCVLDLNGDGLSDDL VGAPMFSEIRDEGQVTVYINR	343
hITA4	346 GSGAVMNAMETNLVGSDKYAARFGESIVNLGDIDNDFEDVAIGAPQEDD	395
hITA9	344 GNGALEEQLA--LTGDGAYNAHFGESIASLDDLDNDFPDVAIGAPKEDD	391
hITA4	396 LQGAIYIYNGRADGISSTFSQRIEGLQISKLSMFGQSIGQIDADNNGY	445
hITA9	392 FAGAVYIYHG DAGGIVPQYSMKLSGQKINPVL R MFGQSIGGIDMDGNGY	441
hITA4	446 VDVAVGAFRSDSAVLLRTRPVVIVDASLSHPESVNRKFDCEVNGWPSVC	495
hITA9	442 PDVTVGAFMSDSVLLRARPVITVDVSI FLPGSINITAPQCHDQQPVNC	491
hITA4	496 IDLTLCFYSYKGEVPGYIVL FYNMSLDVNRKAESP-PRFYFSSNG-TSDV	543
hITA9	492 LNVVTCFSFHGKHVPGEIGLNYVLMADVAKKEKGQMPRVYFVLLGETMQ	541
hITA4	544 ITGSIQVSSREANCRTHQAFMRKDVRDILTPIQIEAAYHLGPHVISKRST	593
hITA9	542 VTEKLQLTMEETCRHYVAHVRRVQDVISP I VFEAAYSLS EHVTEGEE-	590
hITA4	594 EEFPLPQPILQKKEKDIMK--TINFARFCAHENC SADLQVSAKIGFLK	641
hITA9	591 RELPPLTPVLRWKKGQKIAQKNQTV-FERNCRSEDCAADLQLQGKLLLS	639
hITA4	642 PHENKTYLAVGSMKTLMLNVSLFNAGDDAYETTLHVKLPVGLYFIKILEL	691
hITA9	640 MDEKTYLALGAVKNIISLNISISNLGDDAYDANVSFNVSRELF FINMWQK	689
hITA4	692 EEKQINCEVTDNSGVVQLDCSIGYIYVDHLSRIDISFLLDVSSLSRAEED	741
hITA9	690 EEMGISCELLESD---FLKCSVGFPMRKSKEYEFSVIFDTS HLSGEEV	736
hITA4	742 LSITVHATCENEEMDNLKHRSRVTVAIPLKYEVKLTVHGFVNPTS FVYGS	791
hITA9	737 LSFI VTAQSGNTERSESLHDNTLVLMVPIMHEVDT SITGIMSPTS FVYGE	786
hITA4	792 N-----DENEPETCMVERMNLTFHVINTGNSMAPNVSV EIMVNSF	832
hITA9	787 SVDAANFIQLDDLE---CHFQPINITLQVYNTGPSTLPGSSVSISFENRL	833

References

1. Patel RB, Dhanesha N, Sutariya B, et al. Targeting Neutrophil alpha9 Improves Functional Outcomes After Stroke in Mice With Obesity-Induced Hyperglycemia. *Stroke*. 2023.
2. Dhanesha N, Jain M, Doddapattar P, Undas A, Chauhan AK. Cellular fibronectin promotes deep vein thrombosis in diet-induced obese mice. *J Thromb Haemost*. 2021;19(3):814-821.
3. Grover SP, Kawano T, Wan J, et al. C1 inhibitor deficiency enhances contact pathway-mediated activation of coagulation and venous thrombosis. *Blood*. 2023;141(19):2390-2401.
4. Mwiza JMN, Lee RH, Paul DS, et al. Both G protein-coupled and immunoreceptor tyrosine-based activation motif receptors mediate venous thrombosis in mice. *Blood*. 2022;139(21):3194-3203.
5. Payne H, Brill A. Stenosis of the Inferior Vena Cava: A Murine Model of Deep Vein Thrombosis. *J Vis Exp*. 2017(130).
6. Diaz JA, Saha P, Cooley B, et al. Choosing a Mouse Model of Venous Thrombosis. *Arterioscler Thromb Vasc Biol*. 2019;39(3):311-318.
7. Dhanesha N, Jain M, Tripathi AK, et al. Targeting Myeloid-Specific Integrin alpha9beta1 Improves Short- and Long-Term Stroke Outcomes in Murine Models With Preexisting Comorbidities by Limiting Thrombosis and Inflammation. *Circ Res*. 2020;126(12):1779-1794.
8. Dhanesha N, Patel RB, Doddapattar P, et al. PKM2 promotes neutrophil activation and cerebral thromboinflammation: therapeutic implications for ischemic stroke. *Blood*. 2022;139(8):1234-1245.
9. Dhanesha N, Ahmad A, Prakash P, Doddapattar P, Lentz SR, Chauhan AK. Genetic Ablation of Extra Domain A of Fibronectin in Hypercholesterolemic Mice Improves Stroke Outcome by Reducing Thrombo-Inflammation. *Circulation*. 2015;132(23):2237-2247.
10. Dhanesha N, Nayak MK, Doddapattar P, et al. Targeting myeloid-cell specific integrin alpha9beta1 inhibits arterial thrombosis in mice. *Blood*. 2020;135(11):857-861.
11. Dobin A, Davis CA, Schlesinger F, et al. STAR: ultrafast universal RNA-seq aligner. *Bioinformatics*. 2013;29(1):15-21.
12. Li B, Dewey CN. RSEM: accurate transcript quantification from RNA-Seq data with or without a reference genome. *BMC Bioinformatics*. 2011;12:323.
13. Ritchie ME, Phipson B, Wu D, et al. powers differential expression analyses for RNA-sequencing and microarray studies. *Nucleic Acids Research*. 2015;43(7).
14. McCarthy DJ, Chen YS, Smyth GK. Differential expression analysis of multifactor RNA-Seq experiments with respect to biological variation. *Nucleic Acids Research*. 2012;40(10):4288-4297.
15. Pilarczyk M, Fazel-Najafabadi M, Kouril M, et al. Connecting omics signatures and revealing biological mechanisms with iLINCS. *Nat Commun*. 2022;13(1):4678.
16. Subramanian A, Narayan R, Corsello SM, et al. A Next Generation Connectivity Map: L1000 Platform and the First 1,000,000 Profiles. *Cell*. 2017;171(6):1437.